New insights into nanomagnetism: spin-polarized scanning tunneling microscopy and spectroscopy studies

Hirofumi Oka, Guillemin Rodary*, Sebastian Wedekind, Pavel A. Ignatiev, Larissa Niebergall, Valeri S. Stepanyuk, Dirk Sander and Jürgen Kirschner

Max-Planck-Institut für Mikrostrukturphysik, Weinberg 2, D-06120 Halle/Saale, Germany

ABSTRACT

We perform low-temperature spin-polarized scanning tunneling microscopy (SP-STM) and spectroscopy measurements in magnetic fields to gain new insights into nanomagnetism. We use the magnetic field to change and control magnetizations of a sample and a magnetic tip, and measure the magnetic hysteresis loops of individual Co nano-islands on Cu(111). We also exploit the high spatial resolution of SP-STM in magnetic fields to measure maps of the differential conductance within a single Co nano-island. In connection with *ab initio* calculations, we find that the spin polarization is not homogeneous but spatially modulated within the nano-island. We ascribe the spatial variation of the spin polarization to spin-dependent electron confinement within the Co nano-island.

Keywords: spin-polarized scanning tunneling microscopy, spin-polarized scanning tunneling spectroscopy, nanomagnetism, Co islands, Cu(111), magnetic hysteresis loop, spin polarization, electron confinement

1. INTRODUCTION

Our desire to make the density of a magnetic storage even higher drives us to explore a fundamental understanding of magnetic properties and spin-dependent phenomena in magnetic nanostructures. To detect, control and manipulate magnetic properties of magnetic nanostructures is a crucial key to the realization of a much higher density of magnetic storage.[1] Spin-polarized scanning tunneling microscopy (SP-STM) and spectroscopy (SP-STS), which exploit the dependence of the tunnel current on the relative orientation between tip and sample magnetizations, the so-called tunnel magnetoresistance effect,[2–4] are powerful techniques in this respect.[5,6] SP-STM and SP-STS have unveiled many aspects of nanomagnetism, surface magnetic structures even down to atomic scale,[7–9] magnetization switching of magnetic nanoislands,[10,11] and the lifetime of an excited spin state in magnetic adatoms.[12]

In this paper, we perform low-temperature SP-STM and SP-STS measurements of Co islands on Cu(111) in magnetic fields. We use the magnetic field to change and control magnetization of a sample and a magnetic tip, and extract the corresponding change of differential tunnel conductance (dI/dV) of the tunnel junction. By plotting the change of dI/dV signal as a function of field, we measure the magnetic hysteresis loops of individual Co nano-islands.[13,14] We also exploit the high spatial resolution of SP-STM in magnetic fields to measure maps of the dI/dV within a single Co nano-island. We find a pronounced spatial modulation of the dI/dV signal within the island due to electron confinement. Remarkably, the amplitude of the dI/dV modulation within the single island strongly depends on magnetization configurations of the island with respect to the magnetic tip. Comparing this experimental results with *ab initio* calculations, we demonstrate that the spin polarization is not homogeneous but spatially modulated within the nano-island. We ascribe the spatial variation of the spin polarization to spin-dependent electron confinement within the Co nano-island.[15–17]

Further author information: (Send correspondence to H.O.)
H.O.: E-mail: oka@mpi-halle.de, Telephone: +49 345 5582 921
*Present address: Laboratoire de Photonique et de Nanostructures, CNRS UPR20, Route de Nozay, 91460 Marcoussis, France

Spintronics IV, edited by Henri-Jean M. Drouhin, Jean-Eric Wegrowe, Manijeh Razeghi,
Proc. of SPIE Vol. 8100, 81000O · © 2011 SPIE · CCC code: 0277-786X/11/$18 · doi: 10.1117/12.892459

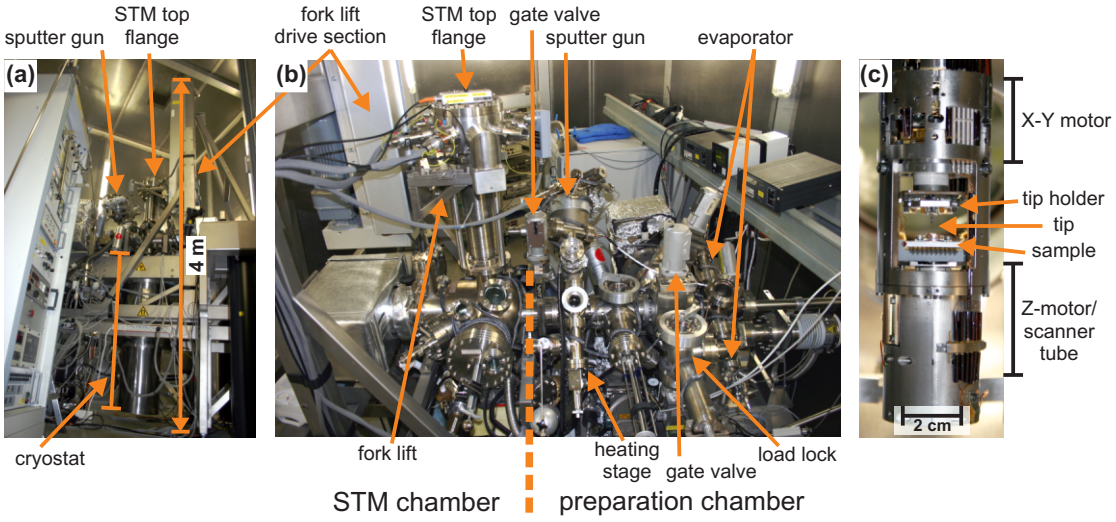

Figure 1. Ultra high vacuum system for low temperature STM in magnetic fields. The STM is cooled by liquid N_2 and liquid He cooled in a bath cryostat. This allows for STM measurements at 7 K in fields of up to 8 T. (a) and (b) Side and top views of the system, respectively. Our system is composed of three chambers separated by gate valves, the STM chamber, the preparation chamber, and the load lock chamber. (c) Head of the STM with tip and sample inserted.

2. EXPERIMENTAL CONDITIONS

2.1 Experimental setup

The results presented in this paper have been obtained with an ultra high vacuum system for low-temperature STM in magnetic fields.[18] Figures 1(a) and 1(b) show side and top views of the system, respectively. The system is composed of three chambers separated by gate valves: the STM chamber, the preparation chamber, and the load lock chamber. The preparation chamber is equipped with a scanning ion gun, a home-built heating stage to heat sample surfaces and tips by electron bombardment, and three e-beam evaporators to deposit different materials onto tips and samples. The STM chamber has a cryostat, which is cooled with liquid N_2 and liquid He and is equipped with a superconducting split coil magnet. It allows to perform STM measurements at 7 K in fields of up to 8 T. The field is oriented perpendicular to the sample surface. The STM head (Fig. 1(c)) is suspended at the lower end of a two-meter long column, which is attached to the STM top flange. By using a fork lift, the STM head can be transfered from or into the cryostat. Thus, *in-situ* sample and tip exchange is possible. The details of the system are given in Ref. 19.

2.2 Preparation and measurement methods

We performed SP-STM measurements on Co islands on Cu(111). Cu(111) substrates were cleaned by cycles of Ar^+ ion sputtering (1 keV, 1.2 μA) and subsequent annealing at 700 K. Submonolayer quantities of Co ($\sim$0.4 ML) were deposited onto the clean Cu(111) surface by an e-beam evaporator at room temperature. Then the sample was immediately transfered into the STM head and cooled down to low temperature in order to avoid intermixing of Co and Cu.[20] Figure 2 is a constant-current STM image showing an overview of Co islands on Cu(111) prepared this way. The Co islands are two atomic layer high ($\sim$0.4 nm) and have a triangular shape.[21,22] The base length of the islands ranges from a few nanometers to 30 nm. W tips, heated to 2100 °C for a few seconds, were used for spin-averaged measurements. Flashed W tip was covered with Cr/Co or Cr layers to get magnetic contrast.[13,14,16]

STM images presented here were measured in the constant current mode with the tunnel current I of order nA and the sample bias voltage V_S in the range -2 – $+2$ V. We measure the differential conductance (dI/dV) by adding an ac modulation signal to the sample bias voltage and detecting the resulting modulated tunnel current by a lock-in amplifier. We exploit two measurement methods to obtain a dI/dV image. One method works with

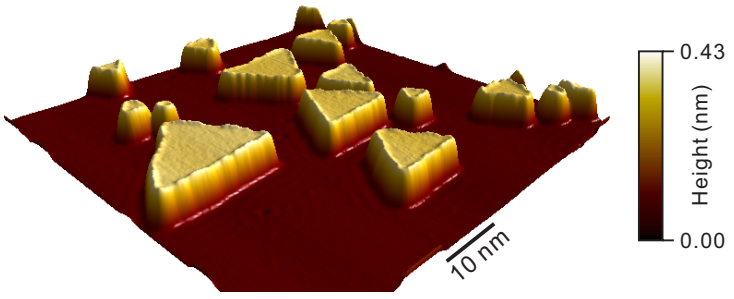

Figure 2. Constant-current STM image of Co islands on Cu(111). ($V_S = -0.1$ V, $I = 1.0$ nA.) Triangular double layer high (∼0.4 nm) Co islands are formed on Cu(111). The islands have a base length from a few nanometers up to 30 nm.

a closed feedback-loop, and the dI/dV image was recorded simultaneously with a constant-current STM image at the tunneling parameters I and V_S. The other method works with an open feedback-loop.

The tip is stabilized at V_{stab} and I_{stab}, and only then the feedback loop is opened. Finally the dI/dV signal is recorded as a function of V. We measure such $dI/dV(V)$ spectra at each pixel of a constant current image to obtain a set of dI/dV images at different bias voltages V.

3. RESULTS AND DISCUSSION

3.1 Magnetic hysteresis loops of individual Co islands

Figure 3(a) shows a constant-current STM image of Co islands on Cu(111). We measure $dI/dV(V)$ spectra at the center of Co islands **A** and **B** in Fig. 3(a). To exclude an effect of position-dependent electronic properties of Co islands on Cu(111),[23,24] all spectra are recorded at the center of the islands. In Fig. 3(b), $dI/dV(V)$ spectra measured on the islands **A** and **B** at different magnetic fields are presented. All spectra show a pronounced peak at -0.3 V, which is ascribed to a localized minority d surface state of Co on Cu(111).[25] The $dI/dV(V)$ signals drastically change with the magnetic fields.

In order to clarify the magnetic field dependent change of the $dI/dV(V)$ signals, we plot $dI/dV(V)$ signals at -0.5 V as a function of field for each island (Fig. 3(c)). The plots in Fig. 3(c) clearly show a symmetric and hysteretic behavior of the $dI/dV(V)$ signal with respect to the field. With increasing the magnetic field from 0 T the $dI/dV(V)$ signal at -0.5 V gradually increases, and at a critical point (1.625 T for the island **A** and 1.250 T for the island **B**) the signal abruptly drops. Then the signal decreases with further increasing the field, and it is saturated around 3 T. With decreasing the magnetic field from 4 T the $dI/dV(V)$ signal gradually increases, and comes back to its original value at 0 T. We observed a similar hysteresis loop of the $dI/dV(V)$ signal for all bias-voltages. The amplitude of the field-induced change depends on the bias voltage, which is apparent from the sets of spectra in Fig. 3(b).

The $dI/dV(V)$ signal with SP-STM depends on the relative orientation of the magnetic tip and sample magnetizations.[5,26] Taking into account that the magnetization direction of the Co islands is aligned along the sample normal, which is an easy magnetization direction of the Co islands on Cu(111),[27] we can ascribe the gradual change of the $dI/dV(V)$ signal to the rotation of the local magnetic moment of the magnetic tip apex in response to the magnetic field.[13] We ascribe the abrupt change of the $dI/dV(V)$ signal at ± 1.625 T and ± 1.250 T to the magnetization switching of the Co islands **A** and **B** along the sample normal, respectively. Schematics in Fig. 3(c) explain magnetization directions of the Co island and the magnetic tip. One might be wondering why Cr covered W tips, which consist of an antiferromagnetic material, follow the applied magnetic field. This can be understood by considering uncompensated spins at the tip apex of Cr tips.[28] STM tips have small clusters at the end, which govern the tunnel current. Therefore, we conclude that an uncompensated magnetic moment at the apex of the Cr tips gives rise to the gradual change of the $dI/dV(V)$ signal in Fig. 3(c). Using this technique we can precisely identify the magnetic configurations of the tip and sample magnetizations, parallel (P) and anti-parallel (AP) states, as indicated in Fig. 3(c). This is a mandatory requirement for investigating the spin-dependent quantum interference discussed in the following section. In addition, the technique allows us to

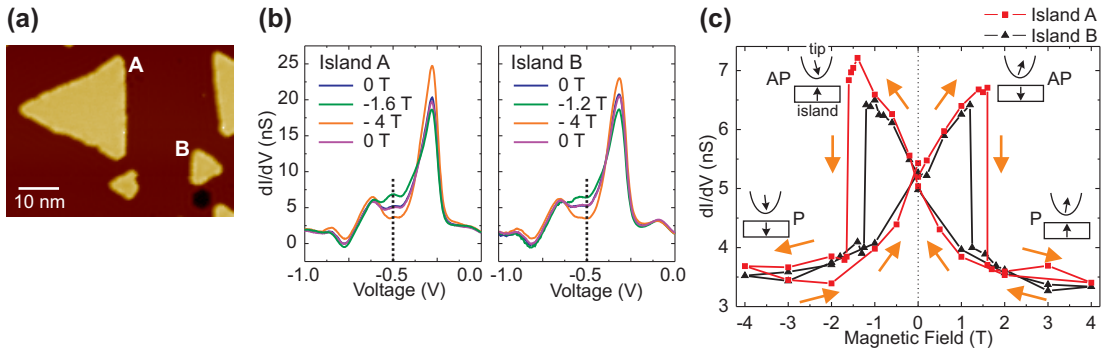

Figure 3. Differential conductance (dI/dV) hysteresis loops of individual Co islands at 7 K. (a) Constant-current STM image of Co islands on Cu(111). ($V_S = -0.51$ V, $I = 1.0$ nA.) (b) dI/dV spectra measured at the center of island **A** and island **B** for different external magnetic fields. ($V_{stab} = +0.5$ V, $I_{stab} = 1.0$ nA.) (c) dI/dV hysteresis loops of islands **A** and **B**. dI/dV signals at $V = -0.5$ V, which is indicated by the dotted lines in (b), are plotted as a function of the magnetic field for each island. Arrows show the direction of the magnetic field sweep. The sudden signal drop indicates a magnetization reversal at 1.250 and 1.625 T for the smaller (**B**) and larger (**A**) island, respectively. Schematics indicate magnetization directions of the Co island and the magnetic tip. P and AP denote parallel and anti-parallel magnetization configurations of the Co island with respect to the magnetic tip. These measurements were done with a Cr-coated W tip.

access to magnetic switching fields of individual magnetic nanostructures. We find that the magnetic switching field depends on the size of the nanostructure.[11, 13, 27]

3.2 Spin-dependent quantum interference within a single Co island

First we present results of quantum interference within Co islands on Cu(111). Figure 4(a) shows a constant-current STM image of a Co island, which has a base length of 19 nm. Figures 4(b)–(e) present a series of dI/dV images of the Co island of Fig. 4(a), measured at different bias voltages. These dI/dV images were measured simultaneously with a constant-current STM image using the close feedback loop method (see Sec. 2.2). For example, Fig. 4(c) and (a) were measured at the same time. We observe pronounced modulation patterns of the dI/dV signal within the Co island. The spatial modulation pattern of the dI/dV signal drastically changes with bias voltage. The dI/dV modulation shows a shorter periodicity with increasing bias voltage.

When electrons are confined to nanostructures, electron waves scattered off the boundaries of the nanostructure interfere and form a standing wave pattern. This gives rise to spatial modulations of the electronic local density of states (LDOS), which have been observed by STM.[29, 30] The modulation observed in the dI/dV images in Fig. 4 is ascribed to electron confinement of a *s-p* surface state of Co.[25] The surface state starts around -0.2 eV below the Fermi level and shows a parabolic dispersion relation.[23, 25] With increasing energy, the wave vector

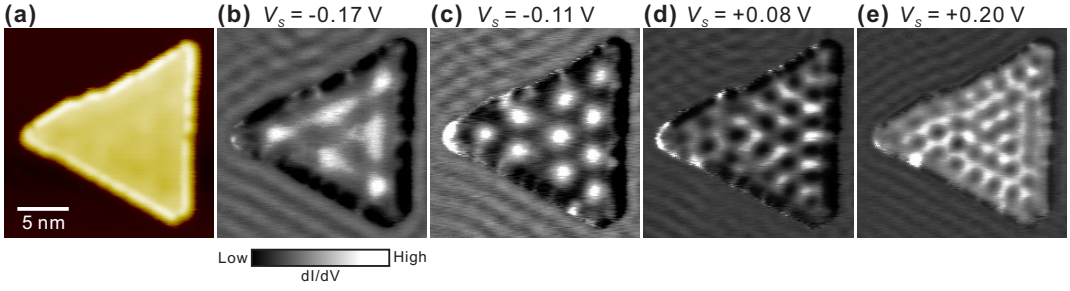

Figure 4. Evolution of electron standing waves on a Co island as a function of energy. (a) Constant-current STM image of a Co island. ($V_S = -0.11$ V, $I = 1.0$ nA.) (b) to (e) dI/dV images of the Co island in (a) recorded at the indicated voltages. The images were measured simultaneously with a constant-current STM image. These measurements were done with a W tip in zero field.

(k) of s-p surface state electrons increases and consequently the wavelength ($\lambda = \pi/k$) of the standing waves decreases. This explains our observations in Fig. 4 well. Figure 4, therefore, reveals that the LDOS within the Co island is spatially modulated due to electron confinement of the s-p surface state. Note that in Figs. 4(b)–(e) a modulation is observed outside the island, on the Cu(111) substrate surface. It is ascribed to the electron quantum interference of s-p surface state electrons of Cu(111).[31]

Next, we perform SP-STM measurements with a Cr/Co covered W tip to investigate spin-dependent electron confinement. Figure 5(a) shows a constant-current STM image of a single Co island on Cu(111). Before measuring a dI/dV image, we record a dI/dV hysteresis loop (not shown) using the technique explained in Sec. 3.1 to characterize the magnetization orientation of the Co island with respect to the magnetic tip. We find that the Co island in Fig. 5(a) exhibits a magnetic switching field of ± 1.3 T (see Ref. 16). We measure two dI/dV images of the Co island with AP and P magnetization configurations of the Co island with respect to the magnetic tip at -1.1 T. These maps are presented in Figs. 5(b) and (c), respectively. Both images were obtained using the open feedback loop method (see Sec. 2.2). The images show a clear LDOS modulation with the same periodicity, but significantly different intensities for AP and P states.

To clarify this difference, we calculate the asymmetry of the dI/dV signal as

$$A_{dI/dV} \equiv \frac{dI/dV_{AP} - dI/dV_P}{dI/dV_{AP} + dI/dV_P}, \tag{1}$$

where dI/dV_{AP} and dI/dV_P are the dI/dV signals measured in the AP and P states, respectively. Figure 5(d) shows a dI/dV asymmetry ($A_{dI/dV}$) map calculated from the two dI/dV images in Fig. 5(b) and (c) using Eq. 1. The $A_{dI/dV}$ around the Fermi level, $V = +0.03$ V, exhibits a pronounced position dependence within the Co island. The Co island exhibits negative $A_{dI/dV}$ values near the edge of the island. In the center region, the island shows positive values and a clear modulation of the $A_{dI/dV}$. The modulation pattern observed in the $A_{dI/dV}$ map (Fig. 5(d)) resembles that of the LDOS in the dI/dV images (Fig. 5(b) and (c)).

The difference in the sign of $A_{dI/dV}$ between near the edge and in the center of the Co island can be explained by a rim state, which is spatially localized around the edges of the Co island.[23] The rim state originates from a minority d state.[23] In contrast, the center region of the island exhibits mainly the opposite spin character around the Fermi level, which is ascribed to a majority s-p surface state.[25] According to theoretical predictions,[26,32] we can link the $A_{dI/dV}$ as defined in Eq. 1 to the spin polarization.

$$A_{dI/dV} = -P_T P_S, \tag{2}$$

where P_T (P_S) is the spin polarization of the tip (sample). We can assume that the spin polarization of the tip, P_T, is constant since the magnetization direction of the tip and the applied bias-voltage are fixed in the two

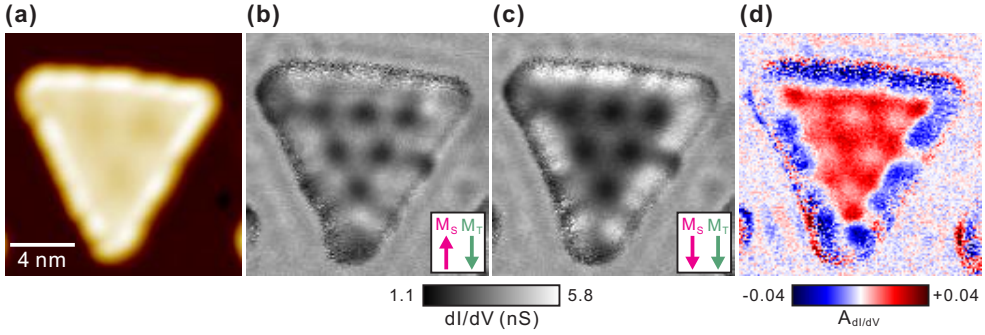

Figure 5. dI/dV-asymmetry map of a single Co island at 8 K. (a) Constant-current STM image of a Co island on Cu(111). ($V_S = -0.1$ V, $I = 1.0$ nA.) (b) and (c) dI/dV images of the Co island in (a). Both images were measured at -1.1 T, but with different relative magnetization orientations between the Co island and the magnetic tip, (b) in AP and (c) in P orientation. ($V = +0.03$ V, $V_{stab} = +0.5$ V, $I_{stab} = 1.0$ nA.) (d) dI/dV-asymmetry map calculated using Eq. 1 from the two dI/dV images in (b) and (c). These measurements were done with a Cr/Co/W tip.

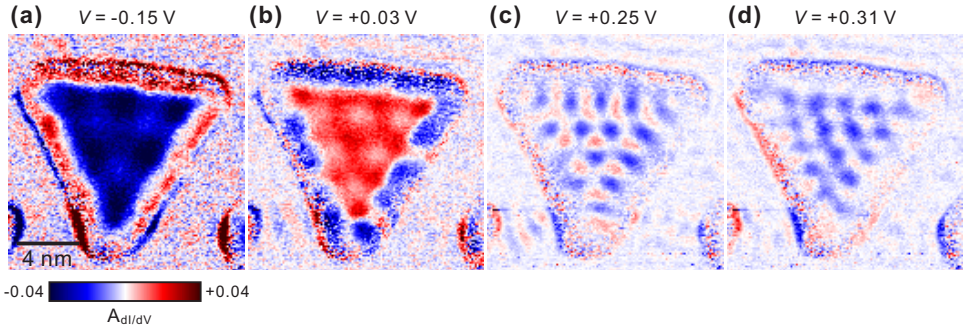

Figure 6. Energy dependence of the dI/dV-asymmetry maps of the Co island at 8 K. (a) to (d) Experimental dI/dV-asymmetry maps obtained on the Co island of Fig. 3(a). The dI/dV-asymmetry maps are calculated using Eq. 1 from two dI/dV images measured at AP and P states. (Measurement conditions of dI/dV images: $V_{stab} = +0.5$ V, $I_{stab} = 1.0$ nA, -1.1 T.)

measurements of the dI/dV image. Thus, $A_{dI/dV}$ reflects the spin polarization of the sample, P_S:

$$A_{dI/dV} \propto P_S. \tag{3}$$

A comparison with density functional calculations confirms this assessment.[16] Therefore, we conclude that a negative $A_{dI/dV}$ near the edge of the island is ascribed to a negative spin polarization of the sample because minority spin electrons originating from the minority d rim state are dominant, and that a positive $A_{dI/dV}$ in the center region is attributed to a positive spin polarization of the sample because majority spin electrons from the majority s-p surface state are dominant.

The modulation observed in the $A_{dI/dV}$ map (Fig. 5(d)) can be interpreted in view of the spin selectivity of electronic quantum confinement.[15] The quantum confinement hardly influences energetically localized electronic states but mainly affects energetically dispersive states. Since the majority s-p surface state is the only dispersive state that Co islands on Cu(111) exhibit around the Fermi level, a modulation of the LDOS occurs mainly for majority spin electrons. Thus the LDOS within a Co island is spatially modulated for majority spin electrons but rather constant for minority spin electrons.[15,16] Therefore, $A_{dI/dV}$, that is, the spin polarization within the Co island, is spatially modulated due to spin-dependent quantum interference.[16]

We investigate the energy dependence of $A_{dI/dV}$ maps of the Co island shown in Fig. 5(a). Figure 6 shows the results. All $A_{dI/dV}$ maps show a clear modulation in the center region of the island. The $A_{dI/dV}$ modulation has a shorter wavelength with increasing bias voltage. This is the same trend we have already discussed in Fig. 4. This similarity can be easily understood since the modulation patterns observed in the spin-averaged data (Fig. 4) as well as in the $A_{dI/dV}$ data is dominated by electron confinement of the s-p surface state. We note that the modulation patterns do not originate from atomic structures since the periodicity of the standing waves in the energy range considered, $\geq$1.5 nm, is much larger than the distance between neighboring Co atoms, $\sim$0.2 nm. We find that the sign of the $A_{dI/dV}$ changes with energy.

To understand this, we perform *ab initio* calculations of the spin-resolved LDOS above a bilayer Co film on Cu(111). Figure 7 presents a plot of the spin-resolved LDOS above the Co film as a function of energy. We find that the dominant spin character is strongly energy-dependent. This needs to be considered to understand the spatial variation of the $A_{dI/dV}$ within the Co island. We use the theory data of Fig. 7 to interpret our experimental data shown in Fig. 6.

Around $E = -0.15$ eV and $+0.30$ eV, the minority spin electron shows higher LDOS than the majority spin electron because energetically localized minority d states exist at $E = -0.25$ and $+0.30$ eV, respectively. These d states are hardly influenced by the electron confinement due to localization. Therefore, the spatially flat LDOS for the minority spin electron is larger than the spatially modulated LDOS for the majority spin electron within the Co island. This results in the negative spin polarization within the island, corresponding to the negative $A_{dI/dV}$ observed in Fig. 6(a) and (d). Around the Fermi level, the majority spin electrons becomes dominant

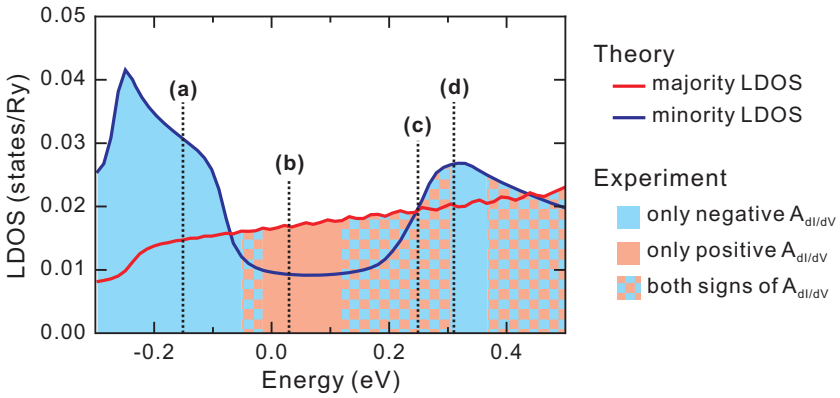

Figure 7. Calculated spin-resolved LDOS of a two-atomic-layer Co film on Cu(111) as a function of energy. Vertical dashed lines mark the energy positions where the dI/dV-asymmetry maps in Fig. 6 are obtained. A color map indicates the energy region where only negative, only positive, or both signs of dI/dV asymmetry are observed in the inner part of the Co island in the experiment.

due to absence of specific electronic states of the minority spin electron. As we already discussed above, the corresponding $A_{dI/dV}$ map in Fig. 6(b) shows the positive value. At $E = +0.25$ eV the LDOS is the same for the majority and the minority spin electron. Here the LDOS of the majority spin electron is not homogeneous but spatially modulated. Therefore, the spatial distribution of the spin polarization is also modulated, and the sign of the spin polarization changes depending on the magnitude of the modulation of the majority spin electron LDOS. This is clearly visible in Fig. 6(c).

We note that with changing bias voltage (Fig. 6(a)–(d)), the $A_{dI/dV}$ at the rim of the island varies. We ascribe this change to the unique electronic properties found at the rim of Co islands.[23] Around the Fermi energy the rim of the island shows a negative spin-polarization as already discussed above, whereas around -0.2 eV the rim area exhibits a positive spin-polarization.[23]

A color map in Fig. 7 indicates the energy span where the experimental $A_{dI/dV}$ map shows only positive, only negative, or both signs of the $A_{dI/dV}$ within the center region of the Co island in Fig. 5(a). It clearly shows that the sign of the $A_{dI/dV}$ and its spatial variation depend on the dominant spin character at a given energy. Our results indicate that the spin-dependent quantum interference causes a spatial modulation of the spin polarization within a magnetic nanostructure, and that local spin polarization within a nanostructure can be controlled by tuning the energy at a given position or the position at a given energy.

4. CONCLUSIONS

We have performed SP-STM measurements on Co islands on Cu(111) in magnetic fields and at low temperature. By exploiting the magnetic field dependence of the dI/dV, we demonstrated that magnetic hysteresis loops of individual nanometer small Co islands can be measured. This technique allows us to access the response of magnetic nanostructures to magnetic fields and to measure magnetic switching fields of individual magnetic nanostructures. This opens a way towards a comprehensive characterization of magnetic properties of individual nanostructures as a function of size, shape, and temperature. These studies will shed new light on magnetic anisotropy and magnetization reversal on the nanoscale.[11] We find that the spin polarization within an individual Co island is spatially modulated due to spin-dependent quantum interference. The finding implies a possible way to control local spin polarization within magnetic nanostructures. The technique of $A_{dI/dV}$ maps allows us to directly image energy-resolved spin polarization maps on nanostructures.

ACKNOWLEDGMENTS

Partial support by Deutsche Forschungsgemeinschaft grant SFB762 is gratefully acknowledged.

REFERENCES

[1] Wolf, S. A., Awschalom, D. D., Buhrman, R. A., Daughton, J. M., Von Molnar, S., Roukes, M. L., Chtchelkanova, A. Y., and Treger, D. M., "Spintronics: A spin-based electronics vision for the future," *Science* **294**(5546), 1488 (2001).

[2] Julliere, M., "Tunneling between ferromagnetic films," *Phys. Lett. A* **54**(3), 225–226 (1975).

[3] Miyazaki, T. and Tezuka, N., "Giant magnetic tunneling effect in $Fe/Al_2O_3/Fe$ junction," *J. Magn. Magn. Mater.* **139**(3), L231–L234 (1995).

[4] Moodera, J. S., Kinder, L. R., Wong, T. M., and Meservey, R., "Large magnetoresistance at room temperature in ferromagnetic thin film tunnel junctions," *Phys. Rev. Lett.* **74**(16), 3273–3276 (1995).

[5] Bode, M., "Spin-polarized scanning tunnelling microscopy," *Rep. Prog. Phys.* **66**, 523 (2003).

[6] Wulfhekel, W. and Kirschner, J., "Spin-polarized scanning tunneling microscopy of magnetic structures and antiferromagnetic thin films," *Annu. Rev. Mater. Res.* **37**, 69–91 (2007).

[7] Bode, M., Getzlaff, M., and Wiesendanger, R., "Spin-polarized vacuum tunneling into the exchange-split surface state of Gd(0001)," *Phys. Rev. Lett.* **81**(19), 4256–4259 (1998).

[8] Heinze, S., Bode, M., Kubetzka, A., Pietzsch, O., Nie, X., Blügel, S., and Wiesendanger, R., "Real-space imaging of two-dimensional antiferromagnetism on the atomic scale," *Science* **288**(5472), 1805 (2000).

[9] Gao, C. L., Wulfhekel, W., and Kirschner, J., "Revealing the 120° antiferromagnetic Néel structure in real space: One monolayer Mn on Ag(111)," *Phys. Rev. Lett.* **101**(26), 267205 (2008).

[10] Bode, M., Pietzsch, O., Kubetzka, A., and Wiesendanger, R., "Shape-dependent thermal switching behavior of superparamagnetic nanoislands," *Phys. Rev. Lett.* **92**(6), 67201 (2004).

[11] Wedekind, S., Rodary, G., Borme, J., Ouazi, S., Nahas, Y., Corbetta, M., Oka, H., Sander, D., and Kirschner, J. *IEEE Trans. Mag.*, (in press).

[12] Loth, S., Etzkorn, M., Lutz, C. P., Eigler, D. M., and Heinrich, A. J., "Measurement of fast electron spin relaxation times with atomic resolution," *Science* **329**(5999), 1628 (2010).

[13] Rodary, G., Wedekind, S., Sander, D., and Kirschner, J., "Magnetic hysteresis loop of single Co nanoislands," *Jpn. J. Appl. Phys.* **47**(12), 9013–9015 (2008).

[14] Rodary, G., Wedekind, S., Oka, H., Sander, D., and Kirschner, J., "Characterization of tips for spin-polarized scanning tunneling microscopy," *Appl. Phys. Lett.* **95**(15), 152513 (2009).

[15] Niebergall, L., Stepanyuk, V. S., Berakdar, J., and Bruno, P., "Controlling the spin polarization of nanostructures on magnetic substrates," *Phys. Rev. Lett.* **96**(12), 127204 (2006).

[16] Oka, H., Ignatiev, P. A., Wedekind, S., Rodary, G., Niebergall, L., Stepanyuk, V. S., Sander, D., and Kirschner, J., "Spin-dependent quantum interference within a single magnetic nanostructure," *Science* **327**(5967), 843 (2010).

[17] Oka, H., Ignatiev, P. A., Wedekind, S., Rodary, G., Niebergall, L., Stepanyuk, V. S., Sander, D., and Kirschner, J., "Spatial modulation of spin polarization within a single Co island," *Hyomen Kagaku* **31**(9), 480 (2010). (in Japanese).

[18] Cryogenic SFM from Omicron NanoTechnology. www.omicron.de.

[19] Wedekind, S., *A spin-polarized scanning tunneling microscopy and spectroscopy study of individual nanoscale particles grown on copper surfaces*, PhD thesis, Martin-Luther-Universität Halle-Wittenberg (2010).

[20] Rabe, A., Memmel, N., Steltenpohl, A., and Fauster, T., "Room-temperature instability of Co/Cu(111)," *Phys. Rev. Lett.* **73**(20), 2728–2731 (1994).

[21] de la Figuera, J., Prieto, J. E., Ocal, C., and Miranda, R., "Scanning-tunneling-microscopy study of the growth of cobalt on Cu(111)," *Phys. Rev. B* **47**(19), 13043–13046 (1993).

[22] Negulyaev, N. N., Stepanyuk, V. S., Bruno, P., Diekhöner, L., Wahl, P., and Kern, K., "Bilayer growth of nanoscale Co islands on Cu(111)," *Phys. Rev. B* **77**(12), 125437 (2008).

[23] Pietzsch, O., Okatov, S., Kubetzka, A., Bode, M., Heinze, S., Lichtenstein, A., and Wiesendanger, R., "Spin-resolved electronic structure of nanoscale cobalt islands on Cu(111)," *Phys. Rev. Lett.* **96**(23), 237203 (2006).

[24] Rastei, M. V., Heinrich, B., Limot, L., Ignatiev, P. A., Stepanyuk, V. S., Bruno, P., and Bucher, J. P., "Size-dependent surface states of strained cobalt nanoislands on Cu(111)," *Phys. Rev. Lett.* **99**(24), 246102 (2007).

[25] Diekhöner, L., Schneider, M. A., Baranov, A. N., Stepanyuk, V. S., Bruno, P., and Kern, K., "Surface states of cobalt nanoislands on Cu(111)," *Phys. Rev. Lett.* **90**(23), 236801 (2003).

[26] Wortmann, D., Heinze, S., Kurz, P., Bihlmayer, G., and Blügel, S., "Resolving complex atomic-scale spin structures by spin-polarized scanning tunneling microscopy," *Phys. Rev. Lett.* **86**(18), 4132–4135 (2001).

[27] Pietzsch, O., Kubetzka, A., Bode, M., and Wiesendanger, R., "Spin-polarized scanning tunneling spectroscopy of nanoscale cobalt islands on Cu(111)," *Phys. Rev. Lett.* **92**(5), 57202 (2004).

[28] Czerner, M., Rodary, G., Wedekind, S., Fedorov, D. V., Sander, D., Mertig, I., and Kirschner, J., "Electronic picture of spin-polarized tunneling with a Cr tip," *J. Magn. Magn. Mater.* **322**(9-12), 1416–1418 (2010).

[29] Crommie, M. F., Lutz, C. P., and Eigler, D. M., "Confinement of electrons to quantum corrals on a metal surface," *Science* **262**(5131), 218–220 (1993).

[30] Li, J., Schneider, W. D., Berndt, R., and Crampin, S., "Electron confinement to nanoscale Ag islands on Ag(111): A quantitative study," *Phys. Rev. Lett.* **80**(15), 3332–3335 (1998).

[31] Crommie, M. F., Lutz, C. P., and Eigler, D. M., "Imaging standing waves in a two-dimensional electron gas," *Nature* **363**, 524 (1993).

[32] Tersoff, J. and Hamann, D. R., "Theory and application for the scanning tunneling microscope," *Phys. Rev. Lett.* **50**(25), 1998–2001 (1983).